SolarPACES 2023, 29th International Conference on Concentrating Solar Power, Thermal, and Chemical Energy Systems

Measurement Systems, Devices, and Procedures

https://doi.org/10.52825/solarpaces.v2i.927



Published: 28. Aug 2024

# Notes on Measuring Concentration Ratio Distribution for a Solar Tower Using Moonlight

Minghuan Guo[1,2,3], Zhifeng Wang[1,2,3], Xiliang Zhang[1], Hao Wang[4], Ying Wu[1,2], and Jian Wang[5]

[1] Institute of Electrical Engineering, Chinese Academy of Sciences, China

[2] University of Chinese Academy of Sciences, China

[3] Beijing Engineering Research Center of Solar Thermal Power, China

[4] Tianjin University, China

[5] North China University of Technology, China

*Correspondence: Minghuan Guo, guominghuan@mail.iee.ac.cn

**Abstract.** The authors' original concept of indirect solar flux mapping of a heliostat field measures CRD using a compact stationary array of moonlight illuminometers on the receiver aperture and a reference moonlight illuminometer on the dual-axis moon tracker. Two sets of moonlight concentration experiments (CCD camera + white target; concentrated lunar beam passing across the linear array of illuminators) were carried out on 63 heliostats at Badaling Solar Tower Power Plant in Beijing on a full moon night in 2018. How the sun and moon shapes differ for CRD as light sources on a solar dish is investigated. Solar/lunar CRDs are similar. Another lunar flux mapping model is also presented, allowing different moon shapes to estimate the solar CRD and contribute improvements in extrapolating measured lunar CRDs to a solar tower working with the real Sun by repeated smooth-filtering. In this paper, some unknown factors, effects, and improvements are carefully considered to enhance the CRD measurement accuracy of a solar tower power plant by using moonlight concentration.

**Keywords:** Concentration Ratio Distribution, Moonlight Concentration, Flux Mapping, Solar Tower, Solar Dish, Deep Learning

## 1. Introduction

Measuring solar flux distribution (also called flux mapping) on a large heliostat field receiver is challenging but essential. Generally, measuring methods are divided into categories: the direct and the indirect methods. Current typical indirect measuring methods comprise the moving whiteboard, CCD camera, and heat flux sensors, which are only effective for small receiver apertures [1]. Indirectly, Ho et al. developed the photographic flux mapping method of PHLUX for external central receivers [2], [3]. It took pictures of the Sun and the concentrated solar image on the receiver surface using the same camera settings. The pixel-grey values of the shot images were calibrated to the flux density using the direct normal solar irradiance (DNI), and the solar flux distribution was obtained. The CCD camera and the absorber reflection properties were mainly used, but PHLUX was still not used in practice due to the complicated and changing spatial distribution of surface reflectance. The concept of a real-time flux density monitoring system on external tube receivers jointly developed by DLR and the company of

CSP Services won the SolarPACES Technology Award 2021, and the indirect solar flux measuring system was mainly composed of a digital camera, reflective properties of the receiver surface, and the reference radiometer [4], [5]. This solar flux mapping technology seems good but is still not widely used. Previous methods of solar concentrators have been limited to using only the Sun or the full moon.

Indirectly, the lunar flux mapping in this study measured the illuminance distribution on the receiver aperture and the direct normal lunar illuminance during moonlight concentration experiments to determine the concentration ratio distribution (CRD). The moonlight concentration experiments were conducted at the Dahan solar power tower plant in Beijing on a full moon night in 2018 and measured illuminance distribution on the receiver aperture using a stationary array of illuminometers and the direct normal lunar illuminance ($DNI_{moon}$) using a reference illuminometer on the dual-axis moon tracker [6]. The solar flux density was estimated as

$$F(x,y) = CR(x,y)_{moon} \bullet DNI_{sun} \quad (1)$$

with the assumption that the lunar CRD be equal to the solar CRD, i.e.,

$$CR(x,y)_{sun} = CR(x,y)_{moon} = I(x,y) / DNI_{moon}\,, \quad (2)$$

where $I(x,y)$ is the illuminance distribution. However, the accuracy of CRD measurement in this lunar flux mapping test was not investigated further.

To indirectly measure the CRD of the solar tower concentrator by concentrating moonlight, a solar dish concentrator was built as an optical stable point-focusing system in the Dahan heliostat field in Beijing. Solar and lunar concentration experiments were carried out to investigate the effect of moon shapes on CRD. A new raytracing simulation model for the moonlight CRD of the dish concentrator was presented. The applicability of lunar flux mapping was expanded over the lunar cycle by allowing different moon shapes [7]. Another lunar flux mapping model was developed to better estimate the expected solar CRD. They contributed improvements in extrapolating measured lunar CRDs to a solar concentrator working with the real Sun [8]. This lunar flux mapping model was applied to a real solar dish concentrator and was most probably applicable to large-scale tower power plants, recognizing the potential of a solar concentrator to enhance the similarity between the solar CRD and a lunar CRD and compensating the residual differences by using repeatedly smoothing filtering of a lunar CRD. Further research is still going on.

# 2. Further considerations and improvements

## 2.1 One simple processing of CRD images

The preliminary lunar flux mapping model does not provide an exact criterion for determining the number N of smooth-filtering operations [8]. It is clear that N increases when the moon phase decreases and that the bigger moon needs fewer smooth-filtering operations on the lunar CRD. Here, a straightforward processing of CRD images for the number N of smooth-filtering operations is presented, as Tab.1 shows.

***Table 1.*** *Sooth-filtering times vs. ratio of the current moon to the full moon*

| **proportion range of moon phase to full Moon (%)** | **Smooth-filtering times (N)** |
|---|---|
| (97.5,100] | 1 |
| (92.5, 97.5] | 2 |
| (87.5, 92.5] | 3 |
| (82.5, 87.5] | 4 |
| (77.5, 82.5] | 5 |
| (72.5, 77.5] | 6 |
| (67.5, 72.5] | 7 |
| (62.5, 67.5] | 8 |
| (57.5, 62.5] | 9 |
| (52.5, 57.5] | 10 |
| (47.5, 52.5] | 11 |
| (42.5, 47.5] | 12 |

## 2.2 Moon size effect

The angular diameter of the moon ($d_{moon}$) viewed from the earth, changes between the small and the supermoons, and the supermoon appears 14% bigger and 30% brighter than the small moon. Thus, the effect of the moon's size is significant to the lunar flux mapping. Therefore, N times of smoothing filtering of a digital lunar CRD to approximate the expected solar CRD should be refined and rewritten as

$$CR_{sun}(x,y) = F(x,y) / DNI_{sun} \quad (3)$$

$$CR(x,y)_{moon} = I(x,y) / DNI_{moon} \quad (4)$$

$$CR_0(x,y) = CR_{moon}(\hat{\sigma}x,\hat{\sigma}y), \quad \widehat{\sigma} = d_{moon}/d_{sun} \quad (5)$$

$$T\{CR_0(x,y)\} = \frac{1}{(2M+1)^2}\sum_{i=-M}^{M}\sum_{j=-M}^{M} CR_0(x\text{-}i\delta, y\text{-}j\delta) \quad (6)$$

$$CR_{sun}(x,y) = c \cdot T^N\{CR_0(x,y)\} = c \cdot T^{N-1}\{T\{CR_0(x,y)\}\} \quad (7)$$

Where $c$ is a scalar reserved for the final modulation of the smoothed CRD image, and δ is the pixel width.

## 2.3 Bias effect of Moon shape center

The grayscale moon image by a CCD camera with a telephoto lens is processed and used as a moon shape for the light source. In Fig.1, the analyzed image center (centroid) biases from the reference moon disk center are 0.94 mrad in the horizontal direction and -1.51 mrad in the vertical direction. This bias is equivalent to some tracking error and affects the lunar CRD, so it should be carefully considered.

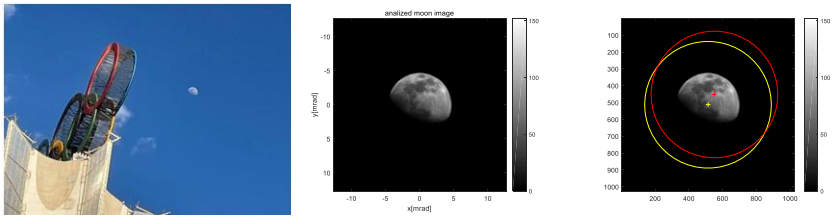


***Figure 1.*** *In Beijing, a moon picture(left), analyzed the moon image(middle) and the center bias on April 30, 2023.*

## 2.4 2-in-1 calibrator for solar CRD from lunar CRDs

Regarding the reserved scalar *c* in Eq. (7) used to modulate a lunar CRD to the expected solar CRD, a compound "2-in-1 calibrator" is designed. Fig. 2 shows the moonlight metering station and the Fresnel point-focusing reflector with small flat mirrors. The Fresnel point-focusing reflector is to produce uniform central flux on the target plane. Initially, the moonlight metering station is configured as a pair of $DNI_{moon}$ measuring sensors, azimuth-elevation dual-axis moon tracker, and the rotational housing dome with a wide window for the moon sighting. Then, the moonlight metering station and the Fresnel point-focusing reflector are combined into the "2-in-1 calibrator", sharing the same dual-axis moon tracker.


***Figure 2**. Moonlight metering station (left), Fresnel point-focusing reflector with small flat mirrors (middle) to produce uniform central flux (right), wholly as the calibrator for solar tower CRD from lunar CRD measurements.*

## 2.5 Heliostat tracking the moon using Sun traces

To make the lunar flux mapping method universal and without modifying the engineering reliable heliostat sun-tracking control programs, the model and algorithm of the heliostat to track the moon at night with the apparent trajectory of the Sun during the day are developed.

The #7.1 heliostat in the Dahan field is taken as an example; the north-east-height coordinates of the heliostat center are (73.546m,27.869m, 5.836m) and the aim point in the target plane on the tower is set as (-74.0m,0m,74.5m). At the local time of 19:27:27, May 2, the control system date and time are changed to 10:00:00, March 21; that is, the time shift is 9.4576h.

As Fig. 3 shows, the tracking effects of the angular residual differences between Sun/Moon traces are further compensated by dynamically modifying the heliostat aim points, which matches the aiming point strategies for solar flux control. This "Sun tracks Moon" model is verified by the moonlight concentration test on the #7.1 heliostat. The details of the "Sun tracks Moon" geometric model, solving algorithms, and the test verifications will be reported in another full paper.

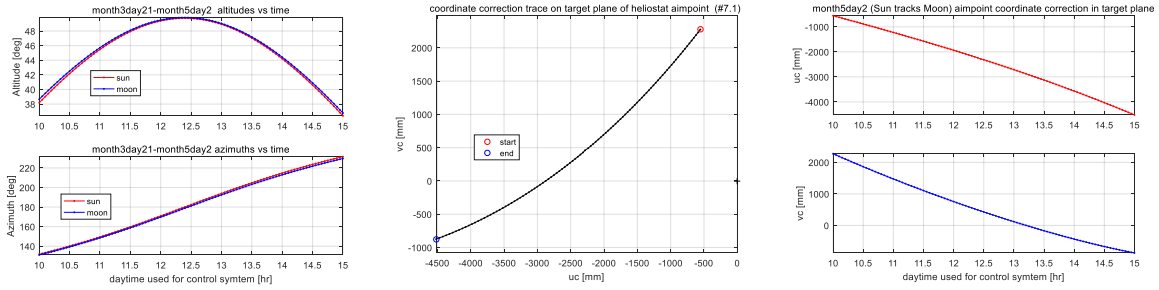


***Figure 3**. Comparison of Sun & Moon position angles (left), Aimpoint correction trace in the target plane (middle), and dynamic aimpoint correction along shifted daytime for May 2, 2023, in Beijing.*

## 2.6 Deep Learning tools used to predict solar CRD images from lunar CRD images

Deep Learning in AI is now fascinating and powerful, and the algorithms are used in many engineering areas. A lot of sunlight and full-moon light concentration experiments on the #7.0 heliostat in the Dahan solar field have been done. A CCD camera takes many solar images on the target plane to generate an adequate dataset for the Deep Learning models. Lunar CRD images are successfully transformed into the solar CRD images of the #7.0 heliostat using the Deep Learning algorithms of CycleGAN and Pix2Pix in Python [9], as Fig.4 shows.

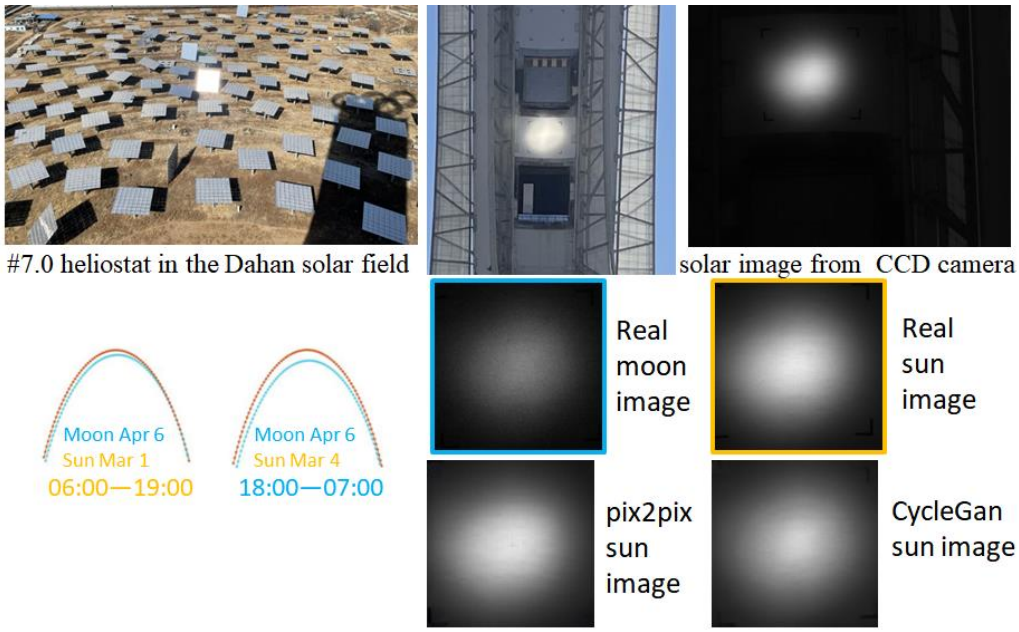


***Figure 4**. Deep Learning is used to predict solar CRD images from lunar CRD images. The upper-left picture is the #7.0 heliostat in the solar field; the upper-middle is a solar image on the target plane; the upper-right is the solar image of the heliostat by a CCD camera set in the solar field; the bottom-left section illustratively shows the comparisons of the sun/moon traces for two different days; the bottom-right section shows four example images in the same size in terms of pixels, and they are the real moon from the CCD camera, the real sun image from the CCD camera, the predicted solar CRD image from the real moon image by the Pix2Pix algorithm, and the predicted solar CRD image from the real moon image by the CycleGAN algorithm, respectively.*

## 3. Conclusions

Following the new lunar flux mapping model for a solar tower system, our authors carefully consider some unknown factors, effects, and improvements to enhance the CRD measurement accuracy of a solar tower power plant by using moonlight concentration:

- Heliostat tracks the moon using Sun traces for engineering reliable and convenient reasons (Sun-track-Moon); residual differences between Sun/Moon traces are further compensated by dynamically modifying the heliostat aim points.
- The moon size and shape center bias effects are considered the newly modeled.
- A 2-in-1 calibrator (Moonlight metering station + Fresnel reflector with flat mirrors) is designed for solar CRD from smoothed lunar CRDs by modulation of the scalar *c* in the new lunar flux model.
- The lunar CRD images have been successfully converted to the solar CRD images of the #7.0 heliostat using the Deep Learning algorithms of CycleGAN and Pix2Pix.

Ongoing work is hard. Cooperations in the community of SolarPACES are welcome.

## Data availability statement

Data can be requested from the authors.

## Author contributions

Minghuan Guo: Conceptualization, Methodology, Formal analysis, Investigation, Writing-original draft, Writing-review & editing, Funding acquisition. Zhifeng Wang: Supervision, Funding acquisition, Project administration, Writing-Reviewing. Xiliang Zhang: Investigation, Mechanical engineering, and drawings. Hao Wang: Investigation, Data curation. Ying Wu: Experiments. Jian Wang: Investigation and experiments.

## Competing interests

The authors declare that they have no competing interests.

## Funding

This work was supported by the National Natural Science Foundation of China Projects (No. 51976058 and No. 61671429).

## Acknowledgement

We like to thank Dr. Feihu Sun, Mrs. Jinping Chen, Dr. Jun Li, Mr. Yi Ruan, Mr. Hong Liu, Mr. Dong Guo, and Mr. Linhao Wang for their kind help in the experiments.

## References

1. A. Ferriere, M. Volut, A. Perez and Y. Volut, "In-situ measurement of concentrated solar flux and distribution at the aperture of a central solar receiver," AIP Conf. Proc., vol. 1734, no.1, 130007, May, 2016, doi: https://doi.org/10.1063/1.4949217.
2. C.K. Ho, S.S. Khalsa and D.D. Gill, "Evaluation of a new tool for heliostat field flux mapping," Proceedings of SolarPACES 2011, SAND2011-5353C, Sep., 2011, https://www.osti.gov/biblio/1140911.
3. C.K. Ho and S.S. Khalsa, "A photographic flux mapping method for concentrating solar collectors and receivers," J. Sol. Energy Eng., vol.134, no.4, 041004 (8 pages), Nov., 2012, doi: https://doi.org/10.1115/1.4006892.
4. C. Raeder, M. Offergeld, M. Roeger, A. Lademann, J. Zoeller, M. Glinka, J. Escamilla and A. Kaempgen, "Proof of concept: Real-time flux density monitoring system on external tube receivers for optimized solar field operation," ICB-REV 2022, Jan., 2023, doi: https://doi.org/10.1063/5.0148725.
5. "SolarPACES Technology Award 2021 for DLR Solar Research and CSP Services." Winners of the 2021 SolarPACES Awards: Technology Innovation Award: DLR Solar Research and CSP Services for their solar flux measurement system. https://www.solarpaces.org/wp-content/uploads/SolarPACES-Award-2021.pdf.
6. M. Guo, X. Wang, N. Wang, F. Sun, X. Zhang and Z. Wang, "Moonlight concentration experiments of Badaling solar tower power plant in Beijing," AIP Conf. Proc., vol. 2303, no.1, 050001, Dec., 2020, doi: https://doi.org/10.1063/5.0028526.
7. H. Wang, M. Guo and Z. Wang, "Calculation model of moonlight concentration ratio distribution for solar dish concentrator," ACTA ENERGIAE SOLARIS SINICA, vol.43, no.9, pp. 148–154, Sept., 2022, doi:https://doi.org/10.19912/j.0254-0096.tynxb.2021-0216.

8. M. Guo, H. Wang, Z. Wang, X. Zhang, F. Sun and N. Wang, "Model for measuring concentration ratio distribution of a dish concentrator using moonlight as a precursor for solar tower flux mapping," AIMS Energy, vol.9, no.4, pp. 727–754, Jun., 2021, https://doi.org/10.3934/energy.2021034.
9. F. Xu, J. Wang, M. Guo, Z. Wang, " Prediction of solar concentration flux distribution for a heliostat based on lunar concentration image and generative adversarial networks," APPLIED ARTIFICIAL INTELLIGENCE, vol.38, no.1, e2332114 (21 pages), Mar. 2024, https://doi.org/10.1080/08839514.2024.2332114.